Distinct host–guest interaction and subdued fluorescence in a coordination network of 2,3,6,7,10,11-hexakis(phenylthio)triphenylene and silver(I) triflate

Kunhao Li[a], Guo Huang[b], Zhengtao Xu[b],*, Patrick J. Carroll[c]

[a]Department of Chemistry, the George Washington University, 725 21st Street NW, Washington, DC 20052, USA
[b]Department of Biology and Chemistry, City University of Hong Kong, 83 Tat Chee Avenue, Kowloon, Hong Kong, PR China
[c]P. Roy and Diana T. Vagelos Laboratories, Department of Chemistry, University of Pennsylvania, 231 South 34th Street, Philadelphia, PA 19104-6323, USA

Abstract

This paper reports our recent efforts in using host–guest interactions to control the fluorescent properties of coordination networks containing polycyclic aromatic units. The polycyclic aromatic ligand 2,3,6,7,10,11-hexakis(phenylthio)triphenylene (HPhTT) coordinates with AgTf (Tf: trifluoromethanesulfonate) in nitrobenzene to form single crystals of a 2-D host network consisting of octameric (i.e., containing eight AgTf units) and dimeric AgTf moieties linked to the HPhTT molecules through the Ag-thioether coordination bonds. The HPhTT adopts a starburst and rather irregular conformation, which apparently contributes to the formation of empty space between the 2-D coordination networks. Such voids are occupied by the nitrobenzene guest molecules, resulting in distinct aromatic–aromatic stacking interactions with the triphenylene units (interplanar distances: 3.46 and 3.60 Å). In comparison to a previous Ag-HPhTT network with toluene as weaker-interacting guests, the current system shows a significantly suppressed fluorescent emission from the triphenylene core, apparently due to the quenching effect from the nitrobenzene guests.
© 2006 Elsevier Inc. All rights reserved.

Keywords: Coordination network; Host–guest chemistry; Polycyclic aromatic hydrocarbon; Fluorescence

1. Introduction

Star-shaped molecules with multiple rigid and functional side arms such as hexakis(phenylthio)benzene (HPhTB, Chart 1) have been originally studied for their versatile ability as hosts to incorporate guest molecules [1,2]. Such ability is apparently derived from the rather open and radiant shapes which tend to obstruct close packing of the molecules, leaving out empty space that can incorporate various guest molecules. Among the numerous related molecules subsequently reported [3–7], highly branched star-shaped molecules have also attracted attentions because of potentially important properties such as electroactivity [8,9], intermolecular recognition [10] and

fluorescent sensing [11]. Notably, star-shaped molecules have also entered into the field of crystalline networks for accessing porous or pocket-containing structures, where a wide range of diffusion or host–guest interaction phenomena could potentially be investigated in the context of extended networks [12–20].

To take advantage of this ability to include guest molecules, and to promote closer and more distinct interactions with the host network, we look to an expanded version of the hexa-host ligands with the triphenylene unit at the core (e.g., molecule HPhTT) (Chart 1).

Due to their relatively large and fused π-electron systems, triphenylene-based molecules has been widely studied for their discotic liquid crystalline properties [21–24], light-emitting materials and as potential organic semiconductors [25,26]. One of the research efforts in this group is to assemble large aromatic fragments such as the
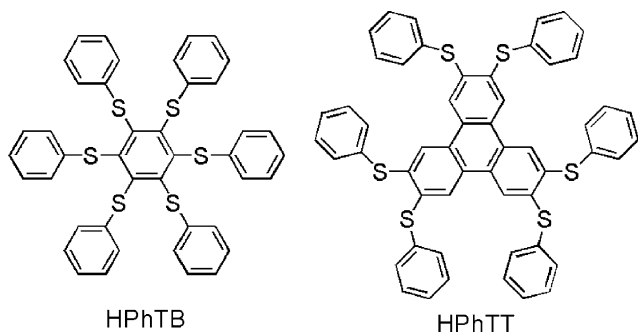

Chart 1.

triphenylene unit into porous metal-organic frameworks. We believe that the large π-electron system of triphenylene units would help impart to the frameworks a wide range of solid-state electronic and fluorescent properties that can be studied in connection with the rich host–guest chemistry associated with star-shaped molecules. Recently, we have reported 1-D and 3-D coordination networks based upon silver (I) triflate (AgTf) and the hexa-host ligand 2,3,6,7,10,11-Hexakis(phenylthio)triphenylene (HPhTT), in which the fluorescent property of the triphenylene core was largely maintained and solvents molecules such as toluene or THF were included [19,20]. The solvent molecules in these systems were, however, remotely located from the fluorescent chromaphore of the triphenylene unit, and their impact on the photophysical properties are therefore not expected to be significant. Herein we report a 2-D hybrid network based on AgTf and the HPhTT molecules, where more distinct and well-defined stacking motifs between the guest molecules (i.e., nitrobenzene) and the triphenylene core have been achieved. The stronger host–guest interactions is also reflected in the substantially subdued fluorescent emission from the triphenylene core, indicating potential sensing applications in future generations of porous systems based on triphenylene cores.

2. Experimental section

Starting materials, reagents and solvents were purchased from commercial sources (Aldrich and Fisher Scientific) and used without further purification. The molecule HPhTT was prepared from a reported procedure [19]. Solution ^{1}H and ^{13}C NMR spectra were taken on a 200 MHz Varian Mercury spectrometer at room temperature with TMS as the internal standard. X-ray diffraction patterns for the bulk samples were collected at room temperature on a Scintag XDS 2000 diffractometer (Cu$K\alpha$, $\lambda = 1.5418$ Å). The powder samples were pressed onto a glass slide for data collection (in air). A 2θ range of 3–40° was collected. Photoluminescence measurements on the solid samples (ground with KBr and pressed into pellets) were performed on a Shimadzu RF-5301PC spectrofluorimeter at ambient temperature.

2.1. X-ray Quality Single Crystals of HPhTT · 5AgTf · 3PhNO₂ · H₂O(1)

A nitrobenzene solution of HPhTT (7.2 mM, 1 mL) was mixed with a nitrobenzene solution of AgTf (10.8 mM, 2 mL) in a vial, and the mixture was transferred into a series of glass tubes (10 mm OD/6 mm ID, about 0.8 mL for each tube). On top of the mixed solutions was sequentially layered nitrobenzene (0.5 mL) and hexane (0.8 mL). The tubes are then sealed and placed upstanding inside a quiet and dark cabinet. Rod-like, colorless crystals suitable for single-crystal X-ray data collection were recovered after about 2 months. The bulk sample can be more readily prepared by directly mixing nitrobenzene solutions of HPhTT and AgTf at a higher concentration [e.g., 15.9 mg (18.1 µmol) of HPhTT in 0.6 mL of nitrobenzene and 23.8 mg (92.6 µmol) of AgTf in 0.6 mL of nitrobenzene]. The solution mixture was allowed to stand overnight before the crystalline precipitate was collected by vacuum filtration and washed with hexane (yield: 37.3 mg, 81% based on HPhTT). X-ray powder diffraction indicated a single phase consistent with the crystal structure obtained from single-crystal dataset (see Fig. S1 in Supporting Information). No significant change in the diffraction profile was observed over a few days, indicating the general air stability of the crystalline sample. Solution ^{1}H NMR (200 MHz, $CD_2Cl_2 : CD_3COCD_3 = 3:1$) supports the crystallographically determined 1:3 ratio of HPhTT and PhNO₂: δ 7.31–7.44 (m, 30 H, HPhTT phenyl H's), 7.55–7.64 (m, 6 H, nitrobenzene H's), 7.72–7.80 (m, 3 H, nitrobenzene H's), 8.06 (s, 6 H, HPhTT triphenylene H's), 8.20–8.25 (m, 6 H, nitrobenzene H's). Further support for the chemical composition was found in the thermogravimetric analysis (TGA, see below).

2.2. X-ray single-crystal diffraction studies of 1

A colorless block with dimensions $0.32 \times 0.27 \times 0.20$ mm³ was placed and optically centered on a Rigaku Mercury CCD area detector using graphite-monochromated Mo-$K\alpha$ radiation ($\lambda = 0.71069$ Å) at 143 K. Rotation images were processed using CrystalClear (Rigaku Corporation, 1999), producing a listing of unaveraged F^2 and $\sigma(F^2)$ values which were then passed to the CrystalStructure program package (Rigaku Corporation Rigaku/MSC, 2002) for further processing and structure solution on a Dell Pentium III computer. A total of 58,180 reflections were measured over the ranges $5 \leqslant 2\theta \leqslant 54.96°$, $-16 \leqslant h \leqslant 16$, $-17 \leqslant k \leqslant 21$, $-28 \leqslant l \leqslant 28$ yielding 19,811 unique reflections ($R_{int} = 0.0205$). The intensity data were corrected for Lorentz and polarization effects and for absorption (minimum and maximum transmission 0.790, 1.000), using REQAB (from Jacobson, R.A. Department of Chemistry, Iowa State University, Ames, IA; private communication, 1994).

The structure was solved by direct methods (SIR97 [27]). Refinement was by full-matrix least squares based on F^2

Table 1
Crystallographic data for **1**

Chemical formula	$C_{77}H_{53}N_3S_{11}O_{22}F_{15}Ag_5$
fw	2549.23
Space group	P-1
a (Å)	12.6584(4)
b (Å)	16.3807(5)
c (Å)	21.9760(7)
α (deg)	83.183(2)
β (deg)	80.714(2)
γ (deg)	88.849(2)
V (Å^3)	4465.3(2)
Z	2
ρ_{calcd} (g/cm^3)	1.896
Wavelength (Å)	0.71069 (Mo$K\alpha$)
Abs coefficient (μ) (cm^{-1})	14.39
R_1[a]	5.72% [I > 2s(I)]
wR_2[b]	15.01% [I > 2s(I)]

[a] $R_1 = \sum \|F_o\| - |F_c\| / \sum (|F_o|)$.
[b] w$R_2 = \{\sum [w(F_o^2 - F_c^2)^2] / \sum [w(F_o^2)^2]\}^{1/2}$.

using SHELXL-97 (G.M. Sheldrick, University of Göttingen, 1997). All reflections were used during refinement (F^2's that were experimentally negative were replaced by $F^2 = 0$). The weighting scheme used was w = $1/[\sigma^2(F_o^2) + 0.0787P^2 + 16.6281P]$, where $P = (F_o^2 + 2F_c^2)/3$. Non-hydrogen atoms were refined anisotropically and hydrogen atoms were refined using a "riding" model. Refinement converged to $R_1 = 0.0572$ and w$R_2 = 0.1501$ for 17515 reflections for which $F > 4\sigma(F)$ and $R_1 = 0.0634$, w$R_2 = 0.1564$ and GOF = 1.032 for all 19811 unique, non-zero reflections and 1136 variables. The maximum Δ/σ in the final cycle of least squares was 0.002 and the two most prominent peaks in the final difference Fourier were +2.478 and −2.040 e/Å^3. Selected crystallographic results are summarized in Table 1, and full details of the crystallographic studies are included in the Supporting Information.

2.3. TGA

TGA was performed on a Pyris TGA-1 instruments under flowing N_2 gas (20 mL/min) and the heating rate was 5 °C/min. The crystalline sample of **1** (prepared as a bulk sample in the above-mentioned procedure) was suction filtered from the mother liquor and rinsed sequentially with 2 mL of benzene and 2 mL of hexane. After being left under suction for another 2 min to further dry off the residual solvents, about 3.5 mg of the collected sample was loaded into the TGA sample holder, and the heating procedure for TGA was at once started.

3. Results and discussions

Compound $HPhTT \cdot 5AgTf \cdot 3PhNO_2 \cdot H_2O$ (**1**) crystallized in the space group P-1 (no. 2) with $a = 12.6584(4)$ Å, $b = 16.3807(5)$ Å, $c = 21.9760(7)$ Å, $\alpha = 83.183(2)°$, $\beta =$ 80.714(2)°, $\gamma = 88.849(2)°$, $V = 4465.3(2)$ Å^3, $Z = 2$. The unit cell contains two centrosymmetrically related organic molecules of HPhTT and two distinct moieties of the silver (I) triflate (AgTf) components (see Fig. 1). The first AgTf moiety (block I) consists of two crystallographically equivalent Ag$^+$ ions (Ag3 in Fig. 1) that are bridged by the two associating triflate anions (i.e., those of S8 in Fig. 1). Each triflate anion engages two of its oxygen atoms in coordinating to the Ag$^+$ atoms (with each O atom bonded to a separate Ag$^+$ ion, Ag–O distances: 2.434 and 2.361 Å), and the overall block features a center of symmetry. The Ag3 ion is also bonded to the sulfur atoms (S6 and S9) from the HPhTT molecule (bonding distances: Ag3–S6, 2.541 Å; Ag3–S9, 2.577 Å), furnishing an overall distorted tetrahedral coordination sphere.

The second moiety of the AgTf component (block II) is more complex and consists of a total of eight Ag$^+$ atoms (i.e., Ag1, Ag2, Ag4 and Ag5 in Fig. 1) connected by eight associating triflate anions (i.e., those of S3, S4, S7 and S11). Like block I, this block of AgTf is also centrosymmetric and the bonding features of the crystallographically unique Ag(I) constituents are described as follows. The Ag1 atom features a distorted tetrahedral coordination geometry, with two Ag–O bonds formed with two triflate anions (those of S3 and S4; corresponding Ag–O distances: 2.286 and 2.239 Å), and two Ag–S bonds formed with the S1 and S2 atoms from an HPhTT molecule (corresponding Ag–S distances: 2.549 and 2.586 Å). Ag2 is coordinated with one oxygen atom from each of the S4, S7 and S11 triflate anions with the corresponding Ag–O distances being 2.567, 2.501 and 2.640 Å; Ag2 also interacts with two oxygen atoms from the S3 triflate anion (Ag–O distances: 2.450, 2.799 Å), and one sulfur atom (S10′) from an HPhTT molecule (Ag–S distance: 2.533 Å), completing a coordination geometry resembling a distorted trigonal prism. Ag4 is five coordinated, with two Ag–O bonds formed with the S3 and S7 triflate anions (Ag–O distances: 2.483, 2.460 Å, respectively), two Ag–S bonds with the HPhTT molecule (distances: Ag4–S5, 2.522 Å; Ag4–S6, 2.919 Å), and one Ag–O bond (length: 2.308 Å) with a water molecule, which was apparently included during the crystallization process. Ag5 features a five-fold coordination, with two Ag–S bonds formed with two sulfur atoms (S9 and S10) from an HPhTT molecule (distances: Ag5–S9, 2.664 Å; Ag5–S10, 2.787 Å), three Ag–O bonds formed with the S7 triflate anion (Ag–O distance: 2.610 Å) and the centrosymmetrically related S11 and S11′ triflate anions (with Ag–O distances being 2.257 and 2.378 Å, respectively).

The overall connectivity of the 2-D network can be conveniently deconstructed into two building blocks. One is the above-mentioned AgTf block of Ag1, Ag2, Ag4 and Ag5 (block II). The other is the composite unit consisting of the AgTf block of Ag3 (block I) and the two associated HPhTT molecules (e.g., through S6 and S9). This composite unit interacts with block II through atoms of S5, S6, S9 and S10, forming a 1-D network, with blocks I and II alternating each other along the b axis. The 1-D nets
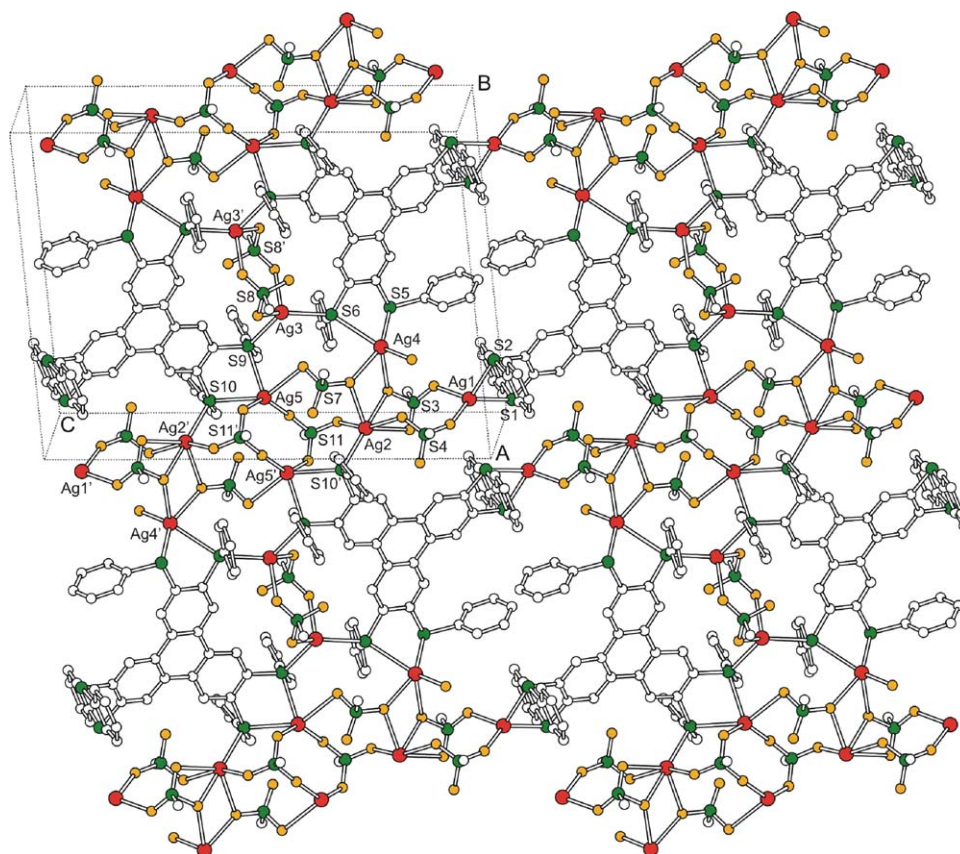
Fig. 1. The 2-D network based on the HPhTT ligand and AgTf in the crystal structure of **1**, with atom labeling for the Ag and S atoms. Green spheres: S; white: C; red: Ag; yellow: O. For clarity, the fluorine atoms of the triflate anion are omitted.

are then integrated into the complete 2-D networks through the chelation between Ag1 and the binding site of the S1 and S2 atoms. The 2-D sheets are packed along the *a*-axis to furnish the overall crystal structure, with no significant bonding interactions found across the individual sheets (see Fig. S2 for a projection of the crystal structure along the *b*-axis).

The substantial voids on both sides of the triphenylene unit are occupied by the guest molecules of nitrobenzene (see Fig. 2, notice also the star-burst and rugged conformation of the HPhTT molecule, which could have been an important factor in generating the empty space). The relative positions of the host and guest molecules are well resolved in the crystal structure (see Figs. 2 and 3, and Fig. S3 in Supporting Information). Each HPhTT molecule is closely associated with two of the nitrobenzene molecules (those of N2 and N3, with interplanar distances being 3.46 and 3.60 Å, respectively), forming the face-to-face stacking on each side of the triphenylene plane. The overlap of the π-electron systems between the triphenylene unit and the two nitrobenzene guests is substantial (see Fig. 3), indicating significant intermolecular interactions between the host framework and the enclusioned guest molecules. By comparison, the third nitrobenzene guest (that of N1) lies about 3.65 Å (interplanar distance) away from the nitrobenzene molecule of N3 (Fig. 3), and it

appear to have much weaker intermolecular (i.e., no aromatic–aromatic stacking) contact with the host network.

The thermogram (see Fig. 4) of the as-synthesized solid sample of **1** features a sharp and distinct step of weight loss of 4.7% around 135 °C, which corresponds to the removal of one nitrobenzene molecule from the crystallographically determined formula HPhTT · 5AgTf · 3PhNO$_2$ · H$_2$O (viz., calculated weight loss due to one nitrobenzene molecule is 4.8%). The next stage of weight loss is less abrupt and extends between 140 and 250 °C. The observed weight loss here is 10.1%, suggesting that the outgoing species may involve the other two nitrobenzene molecules (calculated weight loss due to two nitrobenzene molecules: 9.7%), as well as the water molecule (bound to one of the Ag$^+$ atoms, see crystal structure above; calculated weight loss due to the water molecule: 0.71%). Not surprisingly, these results from TGA closely reflect the different inclusion environments of the guest molecules in the crystal structure of **1**. Thus, the weaker-interacting nitrobenzene molecule (that of N1) can be considered as the nitrobenzene molecule that was first evacuated at about 135 °C, whereas the other nitrobenzene molecules more strongly associated (π-paired) with the triphenylene core may have likely been involved in the ensuing weight loss at the higher temperatures between 140 and 250 °C. X-ray powder
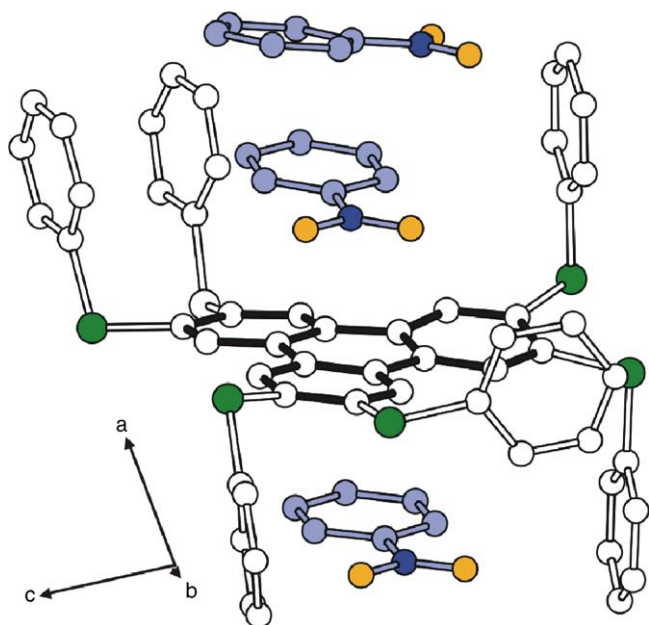
Fig. 2. The HPhTT molecule and the three associated nitrobenzene guests in the crystal structure of **1**. Green spheres: S; yellow spheres: O; dark blue spheres: N; white spheres: C atoms of HPhTT; purple, C atoms of nitrobenzene.
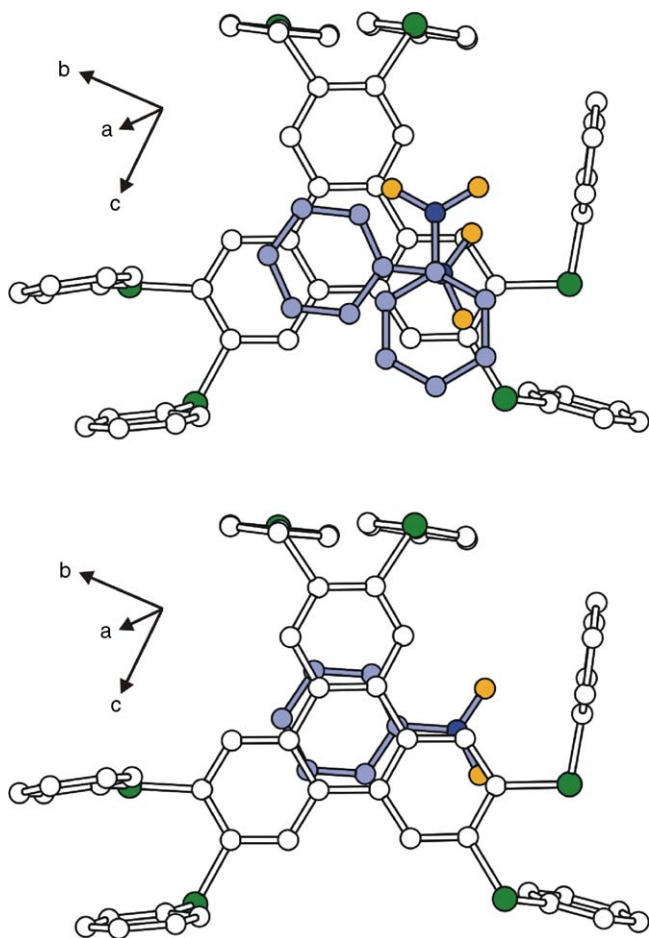

Fig. 3. Top views of the HPhTT molecule and the associated nitrobenzene guests in the crystal structure of **1**.
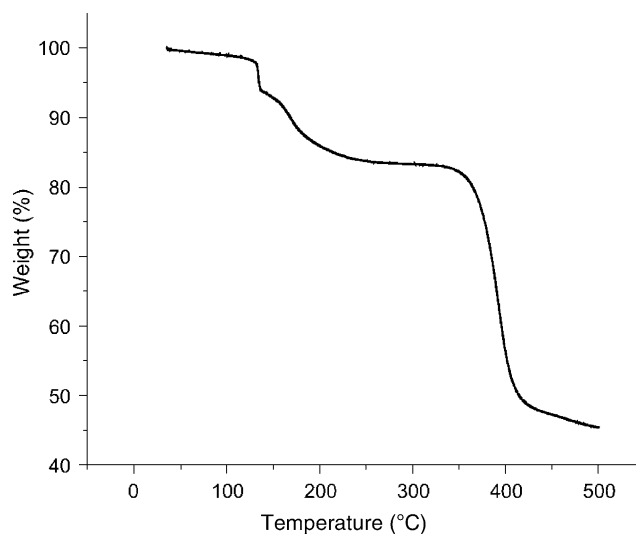

Fig. 4. Thermogram for a solid sample of **1** in a nitrogen atmosphere.

diffraction studies indicate that the evacuation of guest molecules resulted in substantial loss of the crystalline order of the original frameworks. Further studies are ongoing for obtaining higher-dimensional (e.g., 3-D) and more robust frameworks.

Compared with our previously reported AgTf–HPhTT structures containing toluene or tetrahydrofuran as the guest molecules [19], the nitrobenzene-containing structure of **1** thus features more distinct and stronger interactions between the guest molecules and the triphenylene π-system. Such stronger interaction is in line with the electron deficiency of the nitrobenzene molecule, which generally tends to enhance the aromatic–aromatic stacking with an electron-rich aromatic unit such as the triphenylene core in HPhTT. Since the fluorescent properties of the networks would primarily be derived from the triphenylene core, significant impact on the fluorescent property could be expected as a result of the nitrobenzene-triphenylene π-pairing in **1**. To probe the impact of the nitrobenzene guest on the fluorescent properties, a solid sample of **1** (4.8 mg, equivalent to 1.9 μmol of HPhTT) was ground with 100 mg of KBr and pressed into a pellet for fluorescence measurement. Similarly, a pellet consisting of the previously reported 2HPhTT · 3AgTf · 3toluene compound (3.4 mg, equivalent to 2.4 μmol of HPhTT) and 100 mg of KBr was prepared. Solid-state fluorescent spectra of **1** and 2HPhTT · 3AgTf · 3toluene thus obtained indicated substantial suppression of the fluorescent emission intensity in **1**, while the emission wavelength is essentially unchanged (see Fig. 5). Nitrobenzene is usually found to be a solvent that strongly quenches the fluorescence of the solute molecules (see Fig. S4 in Supporting Information). The suppression of fluorescence in the current guest–host structure of **1** is presumably related to the quenching mechanism of nitrobenzene in the solution phase.
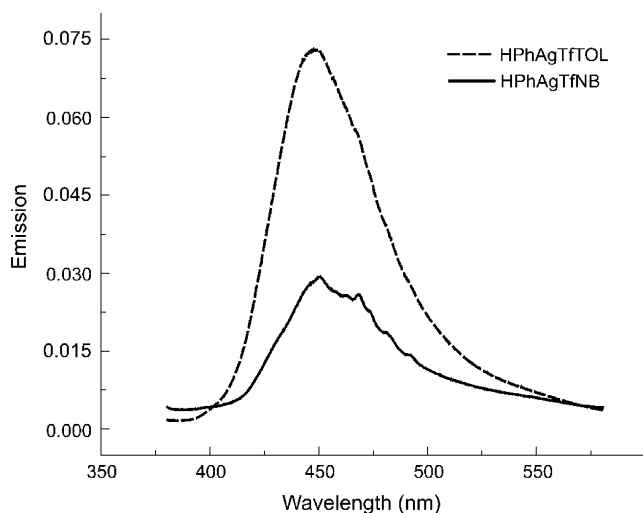
Fig. 5. Room temperature solid-state emission spectra of **1** (solid line) and the previously reported $2HPhTT \cdot 3AgTf \cdot 3toluene$ (dashed line). The excitation wavelength λ_{ex} is 300 nm.

4. Conclusion

In summary, the crystal structure of compound **1** contained a 2-D network based on the coordination bonding between isolated blocks of the silver (I) triflate component and the starburst, triphenylene-based ligand HPhTT. The radiant and rugged shape of the HPhTT molecule apparently helped create empty space for the inclusion of the nitrobenzene molecules as guests in the crystal structure. The nitrobenzene guests form well-defined aromatic–aromatic interactions with the triphenylene units in the host network, and appear to be associated with the substantially suppressed fluorescent emission from the triphenylene units. We now aim for stable 3-D porous networks with polycyclic aromatic units accessible to small-molecule analytes, so as to provide potentially useful materials for applications such as solid-state fluorescent sensing.

Supporting information

Additional figures of the crystal structure of **1**. X-ray powder diffraction patterns for **1**. Full crystallographic data in CIF format for **1**. Solution-state emission spectra for HPhTT. Further details of the crystallographic study. Crystallographic data (excluding structure factors) for the structure(s) reported in this paper have been deposited with the Cambridge Crystallographic Data Centre as supplementary publication no. CCDC 297211. Copies of the data can be obtained free of charge on application to CCDC, 12 Union Road, Cambridge CB2 1EZ, UK (fax: (44) 1223 336-033; e-mail: deposit@ccdc.cam.ac.uk

Appendix A. Supplementary materials

Supplementary data associated with this article can be found in the online version at doi:10.1016/j.jssc.2006.08.005.

References

[1] A.D.U. Hardy, D.D. MacNicol, D.R. Wilson, J. Chem. Soc. Perkin Trans. 2 (1979) 1011–1019.
[2] D.D. MacNicol, P.R. Mallinson, A. Murphy, G.J. Sym, Tetrahedron Lett. 23 (1982) 4131–4134.
[3] M. Gingras, A. Pinchart, C. Dallaire, Angew. Chem. Int. Ed. 37 (1998) 3149–3151.
[4] F.M. Menger, V.A. Azov, J. Am. Chem. Soc. 124 (2002) 11159–11166.
[5] C. Walsdorff, W. Saak, D. Haase, S. Pohl, Chem. Commun. (1997) 1931–1932.
[6] C. Yang, X.-M. Chen, X.-Q. Lu, Q.-H. Zhou, Y.-S. Yang, Chem. Commun. (1997) 2041–2042.
[7] G.H. Grube, E.L. Elliott, R.J. Steffens, C.S. Jones, K.K. Baldridge, J.S. Siegel, Org. Lett. 5 (2003) 713–716.
[8] J.H.R. Tucker, M. Gingras, H. Brand, J.-M. Lehn, J. Chem. Soc. Perkin Trans. 2 (1997) 1303–1307.
[9] M. Gingras, A. Pinchart, C. Dallaire, T. Mallah, E. Levillain, Chem. Eur. J. 10 (2004) 2895–2904.
[10] S. Mizyed, P.E. Georghiou, M. Bancu, B. Cuadra, A.K. Rai, P. Cheng, L.T. Scott, J. Am. Chem. Soc. 123 (2001) 12770–12774.
[11] J. Pang, E.J.P. Marcotte, C. Seward, R.S. Brown, S. Wang, Angew. Chem. Int. Ed. 40 (2001) 4042–4045.
[12] Y. Suenaga, T. Kuroda-Sowa, M. Maekawa, M. Munakata, Dalton Trans. (2000) 3620–3623.
[13] C. Seward, W.-L. Jian, R.-Y. Wang, G.D. Enright, S. Wang, Angew. Chem. Int. Ed. 43 (2004) 2933–2936.
[14] D.M.L. Goodgame, D.A. Grachvogel, A.J.P. White, D.J. Williams, Inorg. Chim. Acta 344 (2003) 214–220.
[15] D.M.L. Goodgame, D.A. Grachvogel, D.J. Williams, Inorg. Chim. Acta 330 (2002) 13–16.
[16] B.F. Hoskins, R. Robson, D.A. Slizys, Angew. Chem. Int. Ed. Engl. 36 (1998) 2752–2755.
[17] K. Kobayashi, T. Shirasaka, A. Sato, E. Horn, N. Furukawa, Angew. Chem. Int. Ed. 38 (1999) 3483–3486.
[18] Y. Suenaga, H. Konaka, K. Kitamura, T. Kuroda-Sowa, M. Maekawa, M. Munakata, Inorg. Chim. Acta 351 (2003) 379–384.
[19] K. Li, Z. Xu, J.C. Fettinger, Inorg. Chem. 43 (2004) 8018–8022.
[20] K. Li, Z. Xu, H. Xu, P.J. Carroll, J.C. Fettinger, Inorg. Chem. 45 (2006) 1032–1037.
[21] J. Billard, J.C. Dubois, N.H. Tinh, A. Zann, Nouv. J. Chim. 2 (1978) 535–540.
[22] W.K. Lee, P.A. Heiney, J.P. McCauley Jr., A.B. Smith III, Mol. Cryst. Liq. Cryst. 198 (1991) 273–284.
[23] C. Destrade, M.C. Mondon, J. Malthete, J. Phys. (Paris) Colloq. 40 (1979) 17–21.

[24] D. Demus, J. Goodby, G.W. Gray, H.W. Spiess, V. Vill, Handbook of Liquid Crystals, vol. 2B, Wiley-VCH Verlag, Weinheim, 1998.

[25] N. Boden, R.J. Bushby, J. Clements, B. Movaghar, K.J. Fonobsn, T. Kreouzis, Phys. Rev. B: Condens. Matter 52 (1995) 13274–13280.

[26] N. Boden, R.J. Bushby, J. Clements, B. Movaghar, J. Mater. Chem. 9 (1999) 2081–2086.

[27] A. Altomare, M.C. Burla, M. Camalli, G.L. Cascarano, C. Giacovazzo, A. Guagliardi, A.G.G. Moliterni, G. Polidori, R. Spagna, J. Appl. Crystallogr. 32 (1999) 115–119.